The Channel Wall Confinement Effect on Periodic Cryogenic Cavitation from the Plano-convex Foil

Yutaka ITO, Tsukasa NAGAYAMA, Hiroshi YAMAUCHI, Takao NAGASAKI
Tokyo Institute of Technology
4259-G3-33, Nagatsuta-cho, Midori-ku, Yokohama, 226-8502, JAPAN
ito@es.titech.ac.jp

Keywords: cavitation, cryogen, visualization, foil, wall confinement effect

Abstract

Flow pattern of cavitation around a plano-convex foil, whose shape is similar to the inducer impeller of the turbo-pumps in the liquid fuel rocket engine, was observed by using a cryogenic cavitation tunnel of blowdown type for visualization. Working fluids were liquid nitrogen and hot water. The parameter range to be varied was between 20 and 60mm for channel width, 20 and 60mm for foil chord, -1.8 and 13.2 for cavitation number, 3.7 and 19.5m/sec for averaged inlet velocity, 8.5×10^4 and 1.5×10^6 for Reynolds number, -8 and 8º for angle of attack, respectively. Especially at positive angle of attack, namely, convex surface being downstream, the whole cavity or a part of the cavity on the foil surface departs periodically. Periodic cavitation occurs only in case of smaller cavitation size than twice foil chord. Cavitation thickness and length in 20mm wide channel are larger than those in 60mm due to the wall confinement effect. Therefore, periodic cavitation in 60mm wide channel easily occurs than that in 20mm. These results suggest that the periodic cavitation is controlled by not only the hydrodynamic effect of vortex shedding but also the channel wall confinement effect.

Introduction

Cavitation is one of the difficult problems to overcome in the recent development of liquid fuel rocket engines, because high performance engines require the higher combustion pressure so that their turbo-pumps have to operate at the higher rotating speed. At the present technology, it is difficult to accurately predict and control the cavitation phenomena and its influence on the performance of the turbo-pumps. Especially, cryogenic cavitation is complex, wherefore cryogens such as LH_2, LOX and LN_2 have three thermodynamic features compared to ordinary fluids like H_2O. Firstly cryogens have small latent heat and nucleation of cavitation easily occurs. Secondly, cryogens are characterized by low specific heat, hence large temperature reduction can result from heat removal due to latent heat of evaporation. Finally, cryogens have steep gradient of the saturation pressure curve, so that the saturation pressure rapidly decreases with the temperature depression, moderating cavitation growth. These are called "thermodynamic effect." Therefore it is not a good way to rely upon existing abundant empirical database of the ordinary fluid pumps in the design for cryogenic ones. Consequently, visible experiments that take into account the thermodynamic effect are required in order to understand the fundamental features and the structure of the cryogenic cavitation in more detail.

Regarding visualization of cavitation around a foil by using water as working fluid, an experimental observation on flows past a plano-convex foil was carried out by Wade et al. [1] in 1966. Their photos of cavitation on the foil were very useful, however, their major aims were to measure lift and drag coefficients of the foil, therefore pressure on the foil surface was not measured. Le et al. [2] reported the difference of cavitation profiles with various angle of attacks (*AOA*) and cavitation numbers (σ) in visible experiments using a plano-convex foil. Kjeldsen et al. [3] classified types and length of cavitation by a combination of *AOA* and σ, and showed the range of periodic cavity departure by using Strouhal number. Franc [4] showed a relationship among cavitation compliance *K*, rate of cavity volume change and rate of local pressure change around a hydrofoil. Furthermore, frequency can be estimated by the cavitation compliance *K* and channel geometry. The relationship he pointed out is very interesting for considering the channel wall confinement effect on periodic cavity departure.

Meanwhile, some cryogenic experiments have been reported for flow configurations other than foils. Hord [5] carried out a visible experimental study on a cavitating flow around a two-dimensional axisymmetric ogive body by using LN_2 and LH_2 in 1974. Thereafter, in order to investigate a faster chocked flow with cavitation in LN_2, LOX and LCH_4, an experimental study using three different shape nozzle was carried out by Simoneau and Hendricks [6] in 1979, who made no effort to visualize the flow patterns. Several U.S. groups [7-10] reported on a subsonic flow of LHe, however measurements were only for pressure or mass flow rate, not elaborating flow visualization. There have been very few studies to visualize cryogenic cavitation, because of difficulty in the experiments. Hori et. al. [11] carried out visualized experiments on the cavitating flow of LN_2 by employing the same nozzle profile as Simoneau and Hendricks. Ishii and Murakami [12] studied the flow of He I and He II in a small nozzle incorporating flow visualization successfully. As mentions above, for the cavitation around foils there are several experiments in case of water flow, but very few in cryogenic flow. One of the objectives in the present study is therefore to investigate the cavitation around the foil in a comparative way of flow visualization

between the cryogen and the ordinary fluids to elucidate the distinction due to the thermodynamic effect. Ito et al. [13] reported flow patterns of cavitation around a foil by using a cryogenic cavitation tunnel as shown in Fig. 1(a). This apparatus consists of upper and lower tanks of 100 and 120 liters capacity, respectively, and an intermediate module of test section of 200 mm length and 20 mm-square cross sectional shape with a 2 inches bore ball valve at the lower end. A foil is set at the center of the test section. The foil is plano-convex with 20 mm chord length, one surface being plane and the other convex with a radius of 26 mm. This profile was chosen because of simplicity, but also of being similar to an inducer impeller in the turbo-pump of rocket engines, which is a primary target of this study. Monitoring the static pressure under operation is provided by a pressure-tap upstream of the foil and two pressure-taps set directly upon the foil surface, whilst two platinum RTDs, i.e. resistance-temperature-detectors, are also installed upstream and downstream of the foil. Two kinds of experimental conditions were arranged to clarify in the first place the effect of σ upon cavitating flows by varying the water temperature under a constant flow velocity, and secondly, the effect of physical (thermodynamic) properties by replacing water into liquid nitrogen under constant flow velocity and σ. The parameter range to be varied is between 0.3 and 12 for σ, 4 and 10 m/sec for inlet flow velocity (u_{in}), and -8° and 8° for *AOA*, respectively. Here, σ were recalculated by using instantaneous velocity, pressure and temperature when snapshots were taken instead of average velocity, pressure and temperature during each experiment as shown in literature 13. In case of cold water (σ = 2.53), small cavitation near the leading edge of the foil was observed to exist at the extreme *AOA* = -8 and 8°, whereas there was no cavitation at other *AOA*s. On the other hand, in cases of hot water (σ = 1.38) and liquid nitrogen (σ = 0.58), cavitation occurred at all the *AOA* settings except 0°. Especially in all cases at positive *AOA*, periodic cavitation departure was observed. It is expected that the periodic cavitation departure is caused by not only the hydrodynamic effect of vortex shedding but also the confinement effect of channel walls. Therefore, new test sections with *W* = 20 mm, 30 mm and 60mm as shown in Fig. 1(b) were fabricated, and other type foils, i.e. triple size foil were tested. By comparing cavitation patterns among these test sections and foil sizes, the condition for the occurrence of periodic cavitation departure is investigated taking into account the wall confinement effect.

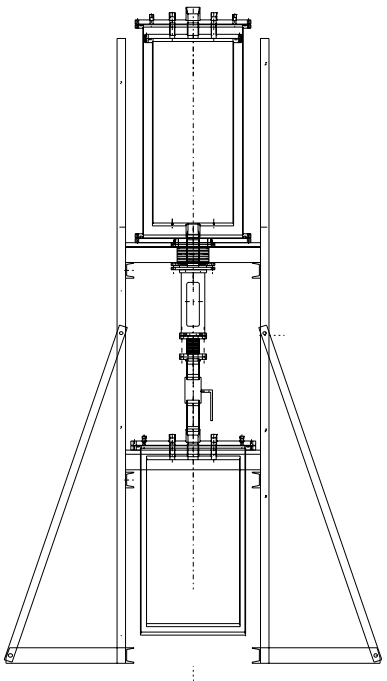

(a)Cryogenic cavitation tunnel of blowdown type

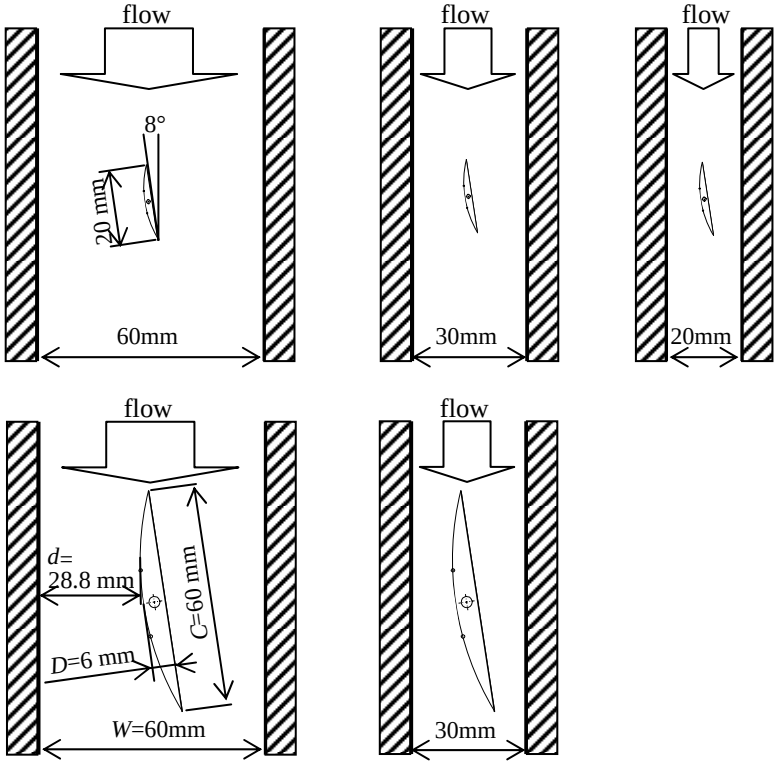

(b)Arrangement and profiles of plano-convex foils and test sections

Fig. 1 Test apparatus

Experimental arrangements

Experimental apparatus

The same cryogenic blowdown tunnel as used in literature 13 was employed except the test section in order to observe the cavitating flow around a foil. Figure 1(b) shows new test sections and the foils geometry. To prevent the failure due to thermal stress more reliably than the old test section, the new ones are made of stainless steel, whilst only the view window is of polycarbonate. The test sections are 288 mm length, 20 mm, 30 mm and 60mm widths and 20mm depth rectangular channels, wherein the foil is set at the center. The foils are two types. First type foil is 20 mm in both chord and span lengths with its shape of the same plano-convex as the previous report[13], that is, one surface being plane and the other convex with a radius of 26 mm. Second type foil is 20 mm in span length, however, 60 mm in chord length with its shape of the triple size plano-convex, that is, the convex surface being in a radius of 78 mm.

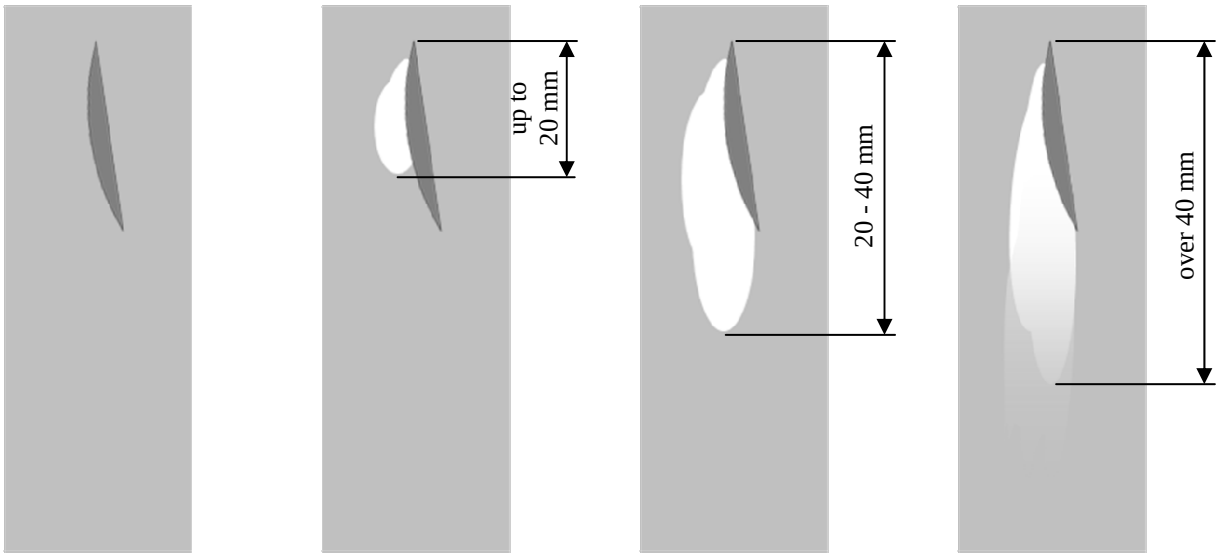

Fig. 2 Cavitaion Size

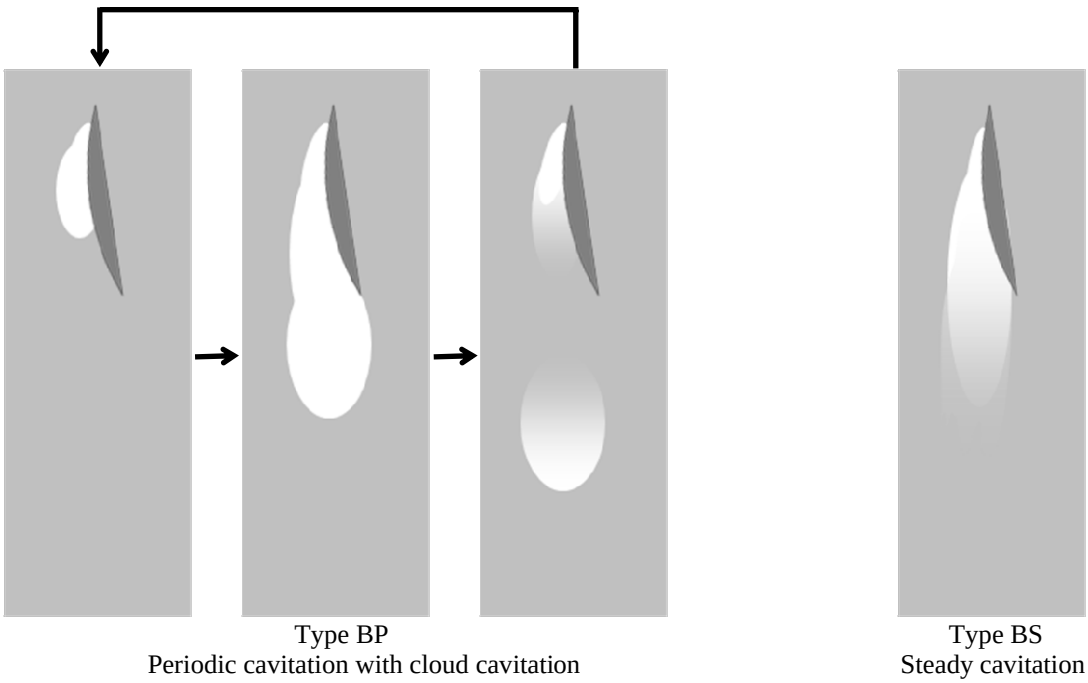

Fig. 3 Cavitaion Patterns

Experimental scheme

Firstly, to elucidate the effect of foil size, i.e. foil chord *C* and foil thickness *D*, a comparison of the results for two foil sizes, that is, a foil with *C*=20mm and *D*=2mm, and that with *C*=60mm and *D*=6mm, was carried out in case of the same 60 mm wide channel. Secondly, in order to clarify the effect of distance *d* between the foil surface and the channel wall, a comparison of the results with channel widths *W* being set among 20 mm, 30 mm and 60 mm in case of the same 20 mm chord foil was carried out. Thirdly, to reveal the effect of inlet velocity u_{in}, a comparison of the results with inlet velocity ranging from 3 to 16 m/sec was carried out. Furthermore, a comparison of the result using hot water with various temperatures and that using liquid nitrogen was carried out. Finally, the mechanism of periodic cavitation departure was discussed.

According to the previous experimental results[13], periodic cavitation departure occurs especially at positive *AOA*, so *AOA* is set at 8° in all cases of this study.

Results and discussion

Cavitation size and patterns

Figure 2 shows a classification of cavitation by means of cavitation size. TypeX indicates no cavitation. TypeA shows small size cavitation with up to 20 mm cavitation length, which is distance from the leading edge of the foil to the end of the time averaged cavitation region. TypeB is the case of middle size cavitation with cavitation length from 20 mm to 40 mm. TypeC means large size cavitation over 40 mm, namely supercavitation. Figure 3 shows cavitation patterns in case of typeB in more detail. TypeBP indicates periodic cavitation with cloud cavitation. Cavity is generated from the mid convex surface and it grows downstream of the trailing edge of the foil. Almost all of the cavity is separated and flowed downward. Hereupon the next cavity is formed again. On the other hand, TypeBS means steady cavitation. The end portion of the cavity, of course, moves frequently, but the cavity can be regarded as steady cavitation on the whole.

Visualization by high-speed video camera

Figure 4 shows pictures taken by high-speed video camera in case of typeA, i.e. small cavitation. TypeA cavitation was observed by using only water as working fluid. Small cavity steadily stays on the convex surface.

Figure 5 shows high-speed video pictures in case of typeBP, i.e. middle size cavitation with periodic cavitation departure. As shown in Fig. 5(a), in water case, the whole cavity departs from the convex surface and there is no cavitation just after departure. On the other hand, as shown in Fig. 5(b), in liquid nitrogen case, upstream portion of the cavity remains on the convex surface after departure. In both cases, departure occurs periodically.

Figure 6 shows pictures in case of typeBS, i.e. middle size steady cavitation. In both cases, the end portion of the cavity irregularly departs, however, the other portion steadily stays.

Figure 7 shows pictures in case of typeC, i.e. large cavitation. As shown in Fig. 7(a), in water case, there is the end section of the cavity out of view. Meanwhile, as shown in Fig. 7(b), in liquid nitrogen case, thicker cavity than that in water case was observed but the end section exists inside of view. These phenomena can be regarded as results caused by thermodynamic effect. Because, thicker cavity in nitrogen was formed due to easier nucleation than that in water, and shorter cavity in nitrogen was obtained due to more suppressed growth than that in water.

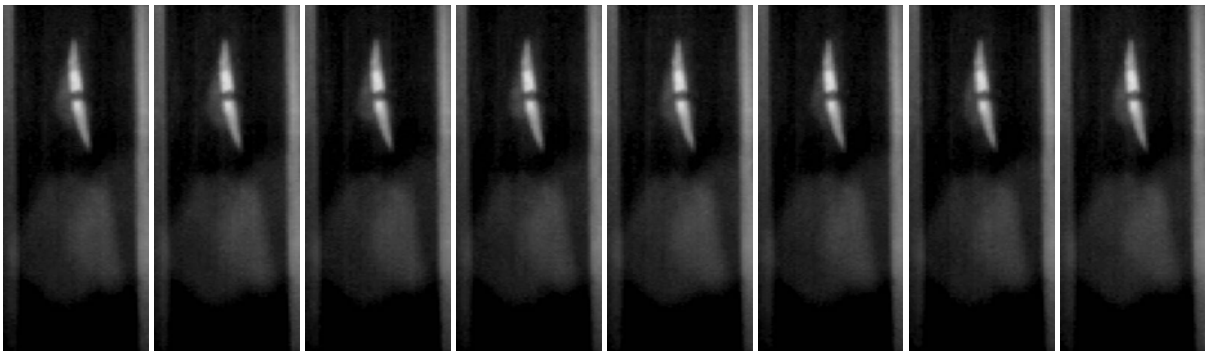

t = 0.0 msec 1.5 msec 3.0 msec 4.5 msec 6.0 msec 7.5 msec 9.0 msec 10.5 msec

water (C = 20 mm, W = 20 mm, T_{in} = 86.9 °C = 360.1 K, u_{in} = 7.0 m/sec, σ = 1.5, Ex. 65)

Fig. 4 Results in case of typeA cavitation

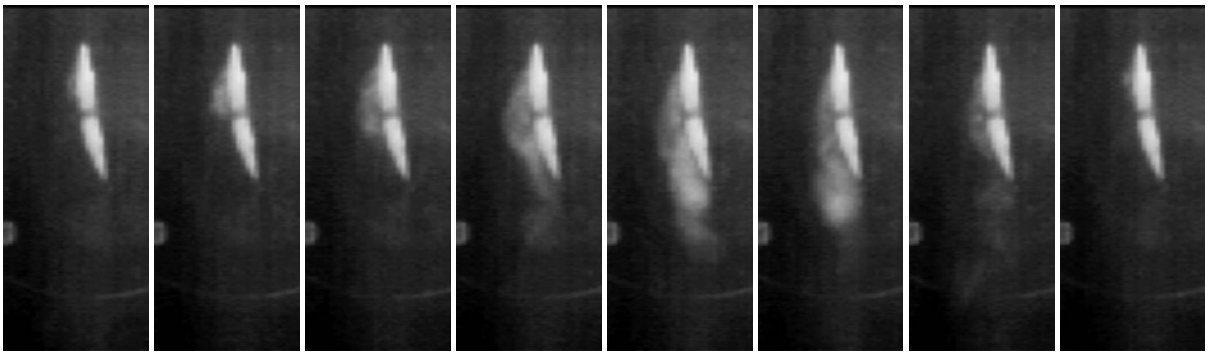

t = 0.0 msec 2.0 msec 4.0 msec 6.0 msec 8.0 msec 10.0 msec 12.0 msec 13.5 msec

(a) water (C = 20 mm, W = 30 mm, T_{in} = 77.9 °C = 351.1 K, u_{in} = 9.9 m/sec, σ = 1.1, Ex. 223)

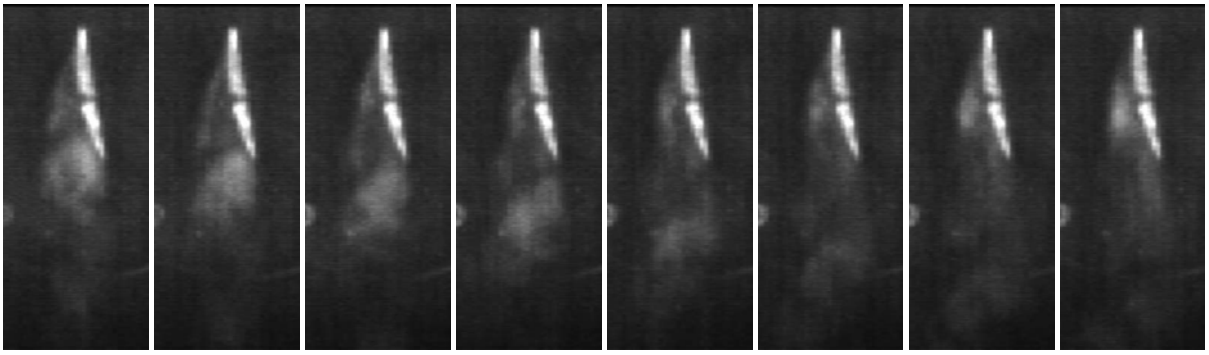

t = 0.0 msec 1.0 msec 2.0 msec 3.0 msec 4.0 msec 5.0 msec 6.0 msec 7.0 msec

(b) liquid nitrogen (C = 20 mm, W = 60 mm, T_{in} = -196.0 °C = 77.15 K, u_{in} = 8.0 m/sec, σ = -0.33, Ex. 272)

Fig. 5 Results in case of typeBP cavitaion

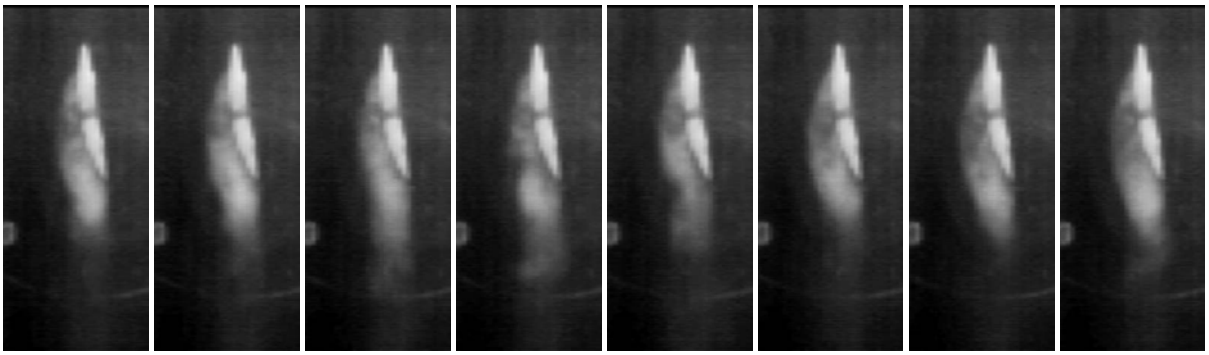

t = 0.0 msec 1.0 msec 2.0 msec 3.0 msec 4.0 msec 5.0 msec 6.0 msec 7.0 msec

(a) water (C = 20 mm, W = 30 mm, T_{in} = 78.0 °C = 351.2 K, u_{in} = 12.4 m/sec, σ = 0.71, Ex. 224)

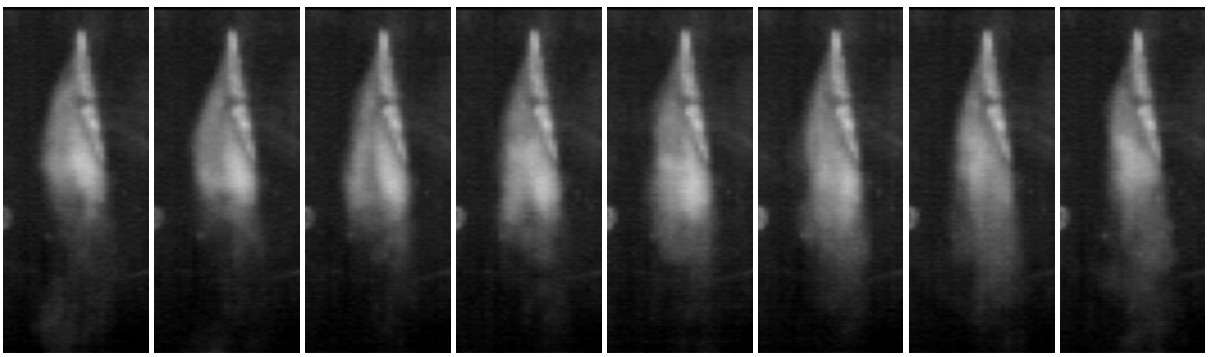

t = 0.0 msec 1.0 msec 2.0 msec 3.0 msec 4.0 msec 5.0 msec 6.0 msec 7.0 msec

(b) liquid nitrogen (C = 20 mm, W = 60 mm, T_{in} = -196.1 °C = 77.1 K, u_{in} = 8.9 m/sec, σ = -0.31, Ex. 269)

Fig. 6 Results in case of typeBS cavitation

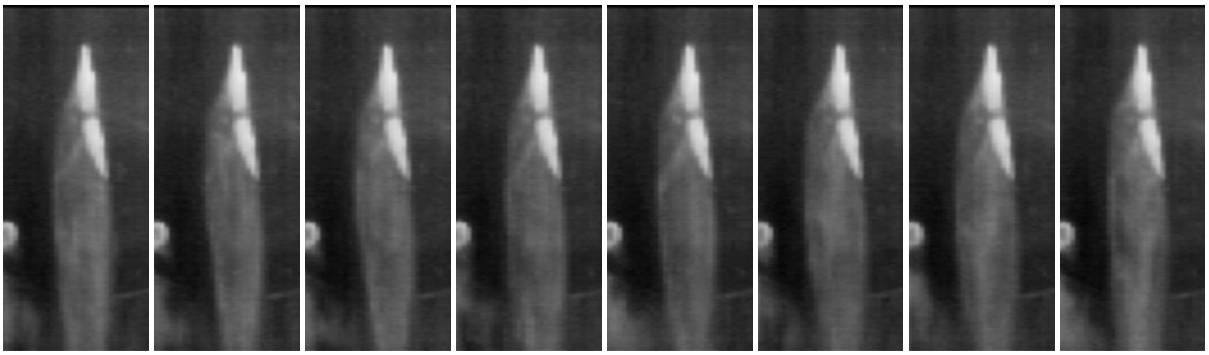

t = 0.0 msec 1.0 msec 2.0 msec 3.0 msec 4.0 msec 5.0 msec 6.0 msec 7.0 msec

(a) water (C = 20 mm, W = 30 mm, T_{in} = 78.0 °C = 351.2 K, u_{in} = 13.9 m/sec, σ = 0.63, Ex. 225)

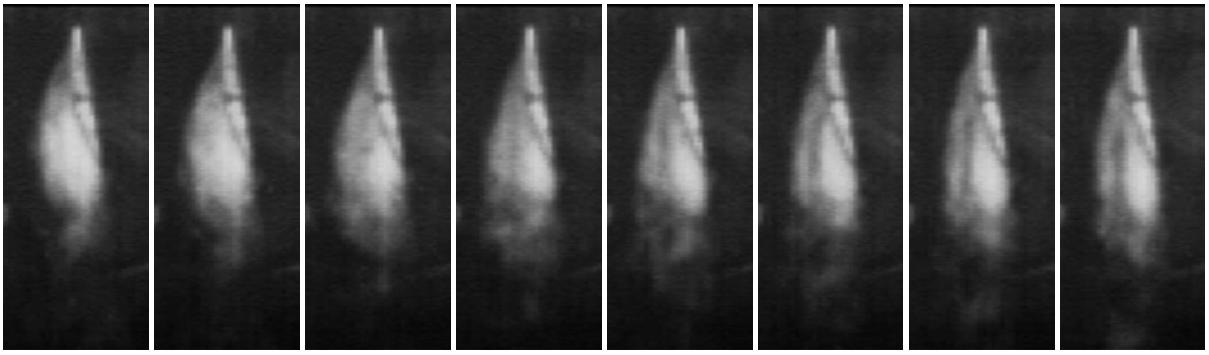

t = 0.0 msec 0.5 msec 1.0 msec 1.5 msec 2.0 msec 2.5 msec 3.0 msec 3.5 msec

(b) liquid nitrogen (C = 20 mm, W = 60 mm, T_{in} = -196.3 °C = 76.9 K, u_{in} = 9.1 m/sec, σ = 0.04, Ex. 268)

Fig. 7 Results in case of typeC cavitation

Cavitation thickness

Due to blockage of the foil, liquid flow around the foil is accelerated, low pressure region is formed and cavitation occurs. Cavity is formed in the low pressure region. As above mentioned, the cavity has four patterns, typeA, typeBP, typeBS and typeC. Especially in case of typeBS and typeC, Maximum thickness was observed at the trailing edge because the cavity steadily covers the trailing edge.

Figure 8 shows maximum thickness in case of typeBS and typeC. Interestingly, maximum thickness is nearly constant for each foil size and each channel width, therefore maximum thickness is decided by only the channel configuration despite the different cavitation number, different temperature, different velocity and even different working fluid.

Effect of foil size

In case of 60 mm wide channel, cavity thickness of 60 mm chord foil is just under three times larger than that of 20 mm foil as seen in Fig. 8.

Effect of distance *d* between the foil surface and the channel wall

In case of 20 mm chord foil, thickness of water cavity approaches to 8 mm with decreasing d from 28.8 mm to 8.8 mm, however, thickness of nitrogen cavity is kept 8 mm with decreasing d. Of course, if the distance between wall and foil surface at trailing edge is smaller than 8mm, cavity thickness is the same as the distance, in other word, the channel between wall and foil is full with cavity.

In case of 60mm chord, thickness of water cavity approaches to 24mm with decreasing d from 26.3 mm to 18.7 mm, however, thickness of nitrogen is held 24 mm with decreasing d. If the distance between wall and foil surface at trailing edge is smaller than 24mm, the channel between wall and foil is full with cavity.

Cavitation pattern distribution

Cavitation patterns are mapped in Fig. 9 with momentum energy $\rho u^2/2$ in abscissa, and pressure difference between the inlet pressure and the saturation pressure for inlet temperature in ordinate. In this figure, iso-cavitation number lines indicate linear lines from the origin of axies. Generally, cavitation type shifts from typeX through typeA, typeBP, typeBS to typeC with decreasing cavitation number. However, cavitation type can not be determined only by cavitation number. For example, in case of σ=0.5, typeC occurs in high speed region, but typeBP occurs in low speed region. When typeBP is focused on, only which has periodic cavity departure, typeBP occurs in the region of lower speed and larger cavitation number than typeBS, but it occurs in higher speed and smaller cavitation number than typeA. When the flow speed is larger than some critical value, say $u^2>13^2$ for LH_2O or $u^2>14^2$ for LN_2, TypeBP does not occur irrespective of pressure difference.

Mechanism of periodic departure

Because of the blockage effect of the foil and the cavity, an adverse pressure gradient is formed. When there is separation behind the foil under the adverse pressure gradient, adverse flow, namely, re-entrant jet

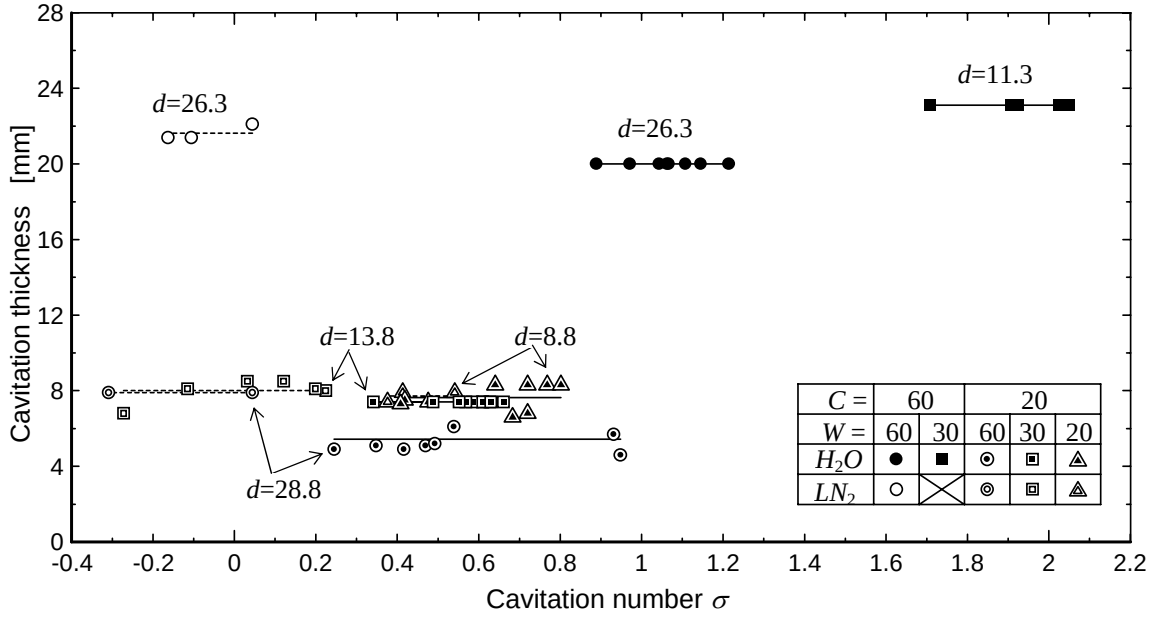

Fig. 8 Cavitation thickness in case of typeBP, typeBS and typeC

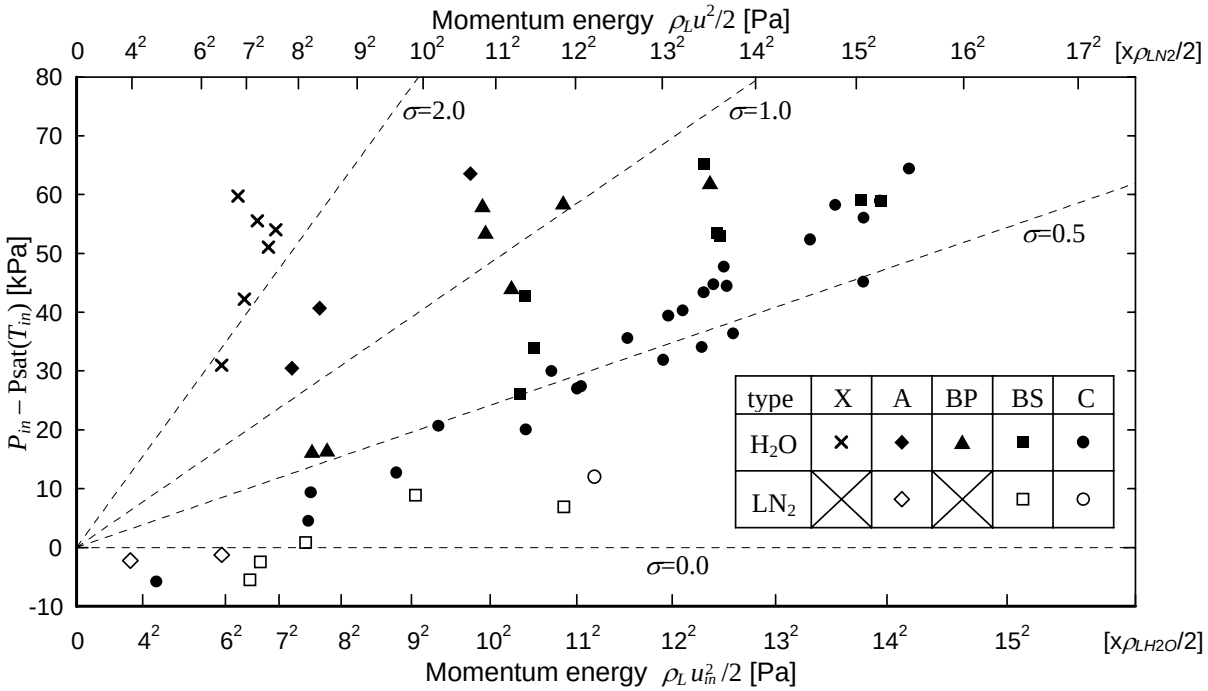

Fig. 9 Cavitation pattern distribution, *C*=20 mm, *W*=30 mm

occurs. The re-entrant jet tears the cavity from the foil surface and the cavity flows downward in case of 60mm wide channel and low speed flow. On the other hand, in case of 30 mm or 20 mm widths channels, because of the narrower width *d* between foil and wall, blockage effect is larger than that in case of 60 mm width. Then pressure reduces and cavity thickness approaches to a constant maximum value with the decease of *d*. When *d* is decreased further, the flow passage on the cavitaion side of the foil is filled with cavity.

Therefore, in case of smaller width between foil and wall, cavitation gushes out of the foil surface and stable cavity stays on the foil surface even with re-entrant jet. This is wall confinement effect.

Furthermore, even in the case of wide channel with 60mm width, when the flow speed is high, pressure also reduces and cavity thickness approaches to

maximum value, so stable cavity stays on the foil surface even with re-entrant jet.

Therefore, periodic cavitation occurs only in case of wide channel and low speed flow.

Conclusion

In order to clarify the cavitation pattern, experiments for visualization by using two kind of plano-convex foil and three kind of wide channel were employed. Caviation pattern can be classified into typeX, typeA, typeBP, typeBS and typeC. Generally, cavitation type shifts from typeX through typeA, typeBP, typeBS to typeC with decreasing cavitation number. TypeBP was observed only in case of wide channel and low speed flow.

Under the same condition, thickness of nitrogen cavity is larger than that of water. Thickness tends to be proportional to the foil size. And there is a maximum cavity thickness for each foil size. Thickness becomes larger approaching to the maximum value with decreasing channel width due to wall confinement effect. When thickness reaches the maximum value, it is kept constant.

References

1) Wade, R. B. and Acosta, A. J.: Experimental observation on the flow past a plano-convex hydrofoil, Transaction of ASME, Journal of Basic Engineering, 1966, pp. 273-283.
2) Le, Q., Franc, J. P. and Michel, J. M.: Partial cavities: Global behaviour and mean pressure distribution, Transaction of ASME, Journal of Fluid Engineering, Vol. 115, 1966, pp. 243-248.
3) Kjeldsen, M., Arndt, R. E. A. and Effertz M.: Investigation od unsteady cavitation phenomena, FEDSM 99-6777, 1999.
4) Franc, J. P.: Partial cavity instabilities and re-entrant jet, CAV2001, lecture. 002, 2001.
5) Hord, J.: Cavitation in Liquid Cryogens II – Hydrofoil. NASA CR 2156, 1974.
6) Simoneau, R. J., Hendricks, R. C: Two-phase choked flow of cryogenic fluids in converging-diverging nozzle, NASA TP 1484, 1979.
7) Ludtk, P. R., Daney, D. E: Cavitation characteristics of a small centrifugal pump in He I and He II, Cryogenics, Vol.28, 1988, pp.96-100.
8) Walstrom, P. L., Weisend II, J. G, Maddocks, J. R., Van Sciver, S. W.: Turbulent flow pressure drop in various He II transfer system components, Cryogenics, Vol.28, 1988, pp.101-109.
9) Daney, D. E.: Cavitation in flowing superfluid helium, Cryogenics, Vol.28, 1988, pp.132-136.
10) Pettersen, M. S., Naud, C., Baliba, S., Maris, H. J.: Experimental observations of cavitation in superfluid helium-4, Physica B, Vol.194-196, 1994, pp.575-576.
11) Hori, S., Ito, Y., Yamaguchi, K.: Observation of Cavitation Bubbles in Cryogenic 2D Nozzle Flows, Proc. of 40th Aerospace Propulsion Conference, 2000, pp.169-174 in Japanese.
12) Ishii, T., Murakami, M: Comparison of cavitating flows in He I and He II, Cryogenics, Vol.43, 2003, pp.507-514.
13) Ito, Y., Sawasaki, K., Tani, N., Nagasaki, T., Nagashima, T.: A Blowdown Cryogenic Cavitation Tunnel and CFD Treatment for Flow Visualization around a Foil, Journal of Thermal Science – International Journal of Thermal and Fluid Sciences, Vol.14, No.4, 2005, pp.346-351.